Imaging lateral heterogeneity at Coronation Field with surface waves

Matthew M. Haney, Boise State University, and Huub Douma, ION Geophysical/GXT Imaging Solutions*

SUMMARY

A longstanding problem in land seismic data processing is the presence of a complex near-surface. We investigate lateral heterogeneity at shallow depths (< 100 m) for a data set from the Coronation Field, Canada, by applying Rayleigh wave group velocity tomography. The 3D-3C data set contains good low frequency content and fundamental mode Rayleigh waves are observed over the frequency band from 3-13 Hz. Group velocity maps over a range of frequencies reveal strong variability in the near-surface. A 3D depth model resulting from this analysis can be used as an initial guess for more advanced imaging methods based on scattered surface waves.

INTRODUCTION

Surface waves do not fit into the prevailing paradigm of reflection seismology: they propagate horizontally, sense the subsurface to depths of only one wavelength, and exhibit velocity dispersion even when anelasticity is negligible. As a result, surface waves are targeted for exclusion from the traditional seismic data processing sequence using methods of surface wave isolation and removal. Although surface waves in the frequency range from 3-30 Hz are not useful for imaging deep ($>$ 100 m) structure, their shallow sensitivity can provide information on the near-surface that is valuable for shear wave statics. Since surface waves propagate laterally, they are particularly well-suited to provide information on long-wavelength statics.

There are many ways to invert for shallow shear velocity structure from observations of surface waves (Xia et al., 1999; Ritzwoller and Levshin, 2002). Perhaps the most popular technique employs linear stacking over an array to measure phase velocity. An advantage of this technique is that accurate timing of the source is not needed and wave modes that do not have linear moveout (e.g., reflections) are attenuated in the stacking process, increasing the signal-to-noise ratio for the surface waves. A disadvantage is that, for a particular frequency, a single phase velocity is estimated over the entire array. Thus, any lateral heterogeneity along the array is “smeared-out” and the subsurface is represented by an effective layered medium. An alternative approach is to estimate group velocity from individual point recordings. In this case, accurate source timing information is necessary; however, since only a single recording is needed, lateral heterogeneity can be estimated through a subsequent application of tomography. Yet another method, known as the HV ratio, inverts for subsurface structure from the spectral ratio of the horizontal and vertical components of a Rayleigh or Scholte wave observed on a 3C receiver (Muyzert, 2007). The HV ratio, or ellipticity (Ross et al., 2008), senses the shallow structure immediately beneath the receiver.

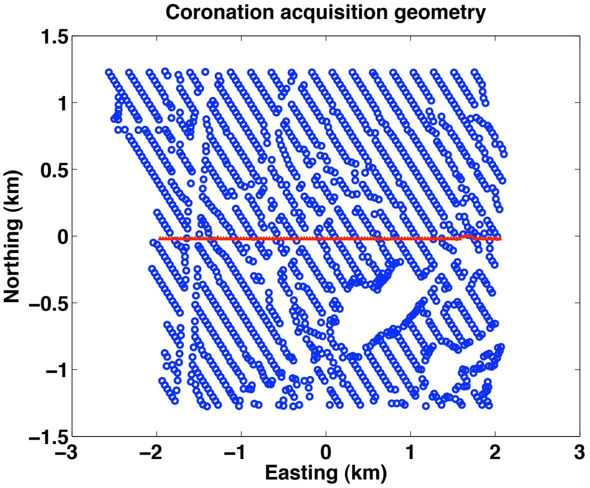

Figure 1: The acquisition geometry of the sources (blue circles) and receivers (red triangles) for the portion of the Coronation data set we analyze here.

We apply Rayleigh wave group velocity tomography to map near-surface structure at the Coronation Field, Canada. Such a technique has been applied before by Abbott et al. (2006) for shallow site characterization. Masterlark et al. (2010) conducted group velocity tomography of Okmok volcano, Alaska, with Rayleigh waves derived from ambient noise and imaged a shallow magma chamber centered beneath the caldera. Recently, Bussat and Kugler (2009) showed that a similar technique can be applied at the reservoir scale in a marine setting. Our purpose is to investigate the ability of surface waves to provide useful information on shear statics, as previously discussed by Ross et al. (2008), instead of being discarded as undesirable noise. We demonstrate how the presence of low frequency surface waves in land seismic data makes it possible to gauge strong variations in shear wave velocity in the shallow subsurface.

DATA AND METHODS

The Coronation data set is a large 3D-3C data set from eastern Alberta, Canada. We plot the acquisition geometry for the portion of the data set we analyze in Figure 1. Source locations, shown as blue circles, are recorded by a single line of 3-component receivers, shown as red triangles. The entire survey covers an area that is roughly 3 km in the north-south direction by 6 km east-west. The number of individual source-receiver pairs in the data set is over 100,000. For 3C data, this brings the total number of data channels to over 300,000. The recording time for the seismic data was 6 s, ensuring that Rayleigh wave arrivals registered even at distant receivers.

The subset of data from the Coronation Field that we analyze is in fact a small portion of the overall data set; we focus on the

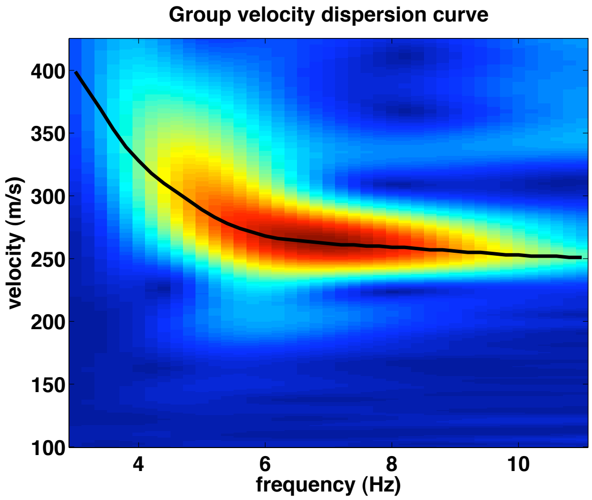

Figure 2: A group velocity dispersion curve for one of the over 100,000 vertical component recordings at the Coronation Field.

recordings of all the sources by a single receiver line, as shown in Figure 1. This means that the lateral resolution of Rayleigh wave group velocity will be best in and around the receiver line. Optimal resolution over a wider area would require the inclusion of additional receiver lines.

In Figure 2, we show a group velocity dispersion curve computed for one of the over 100,000 total vertical component recordings at the Coronation Field. We utilize a multiple-filter technique known as Frequency-Time ANalysis (FTAN) to obtain the dispersion curve (Ritzwoller and Levshin, 2002; Abbott et al., 2006). The dispersion curve is overlain on the group velocity spectrum, a surface defined by the envelopes of a series of narrowband versions of the signal (Abbott et al., 2006). Instead of plotting this surface as a function of traveltime and frequency, the traveltime axis is transformed to a velocity axis since the source-receiver distance is known. The group velocity dispersion curve is then found by tracing the peak power in the group velocity spectrum across the frequency band. To build a group traveltime table over all the traces, the group velocity dispersion curve can be transformed back to group traveltime a function of frequency, again since the the source-receiver distance is known. Note that the dispersion curve in Figure 2 represents the average velocity structure between the source and receiver. In contrast, we obtain *local* dispersion curves after we apply group velocity tomography, as described in a later section.

The dispersion curve in Figure 2 corresponds to the fundamental mode Rayleigh wave. Comparison of the radial trace confirms the existence of the 90 degree phase shift compared to the vertical trace, a hallmark of Rayleigh waves. The dispersion curve extends from 3 to 11 Hz and includes velocities between 250 and 400 m/s. Under the approximation that the phase velocity is equal to the group velocity, we can get a rough estimate of the maximum depth sensitivity of the Rayleigh waves. For the lowest frequency (3 Hz), the velocity of 400 m/s gives a wavelength of 133 m. We can thus expect that a 3D model resulting from tomography and depth inversion of local group velocity dispersion curves will be able to resolve near-surface structure to maximum depths on the order of 100 m.

GROUP TRAVELTIME TABLE

The data processing for surface waves is automated and begins by anti-alias filtering and decimating the vertical component data from a Nyquist frequency of 250 Hz down to 25 Hz. We use the vertical component data since, for an isotropic subsurface, Rayleigh waves are isolated from Love waves on this component. A sample rate of 50 Hz is adequate for analyzing Rayleigh waves between 3 and 13 Hz. We then scan over all source-receiver pairs and form group velocity spectra using FTAN for frequencies from 3-13 Hz. For a single group velocity spectrum from a source-receiver pair, the maximum of the spectrum is selected. From this point, the maximum at each frequency is found in the increasing and decreasing frequency direction away from the global maximum until the amplitude of the maxima are one-fourth of the global maximum value. This defines a possible group velocity dispersion curve. Quality control criteria are applied to this possible dispersion curve to establish whether or not it is acceptable. To be accepted, we impose that the dispersion curve must satisfy the following criteria:

- The derivative of the dispersion curve with frequency never exceeds 200 m/s/Hz
- The dispersion curve extends over at least 4 Hz
- The mean of the dispersion curve is less than 500 m/s and greater than 200 m/s

If these criteria are satisfied for a possible dispersion curve, the dispersion curve is transformed to group traveltime as a function of frequency and saved in the group traveltime table for eventual input into group traveltime tomography. The criteria reflect the properties of a desired dispersion curve: it is relatively smooth, extends over a broad frequency band, and has group velocities similar to those commonly observed over the entire survey during interactive data analysis. On average, dispersion curves associated with 20% of the traces qualify for entry into the group traveltime table. This means that approximately 20,000 traveltimes are available for tomography at each frequency.

GROUP VELOCITY TOMOGRAPHY

Once a group traveltime table as a function of source, receiver, and frequency has been built, we perform tomography over all frequencies from 3-13 Hz in steps of 0.2 Hz. The initial guess for the group velocity map at a particular frequency is taken to be homogeneous with a value equal to the average of all group velocity (computed from group traveltime) measurements at that particular frequency. Thus, the initial model is laterally homogeneous.

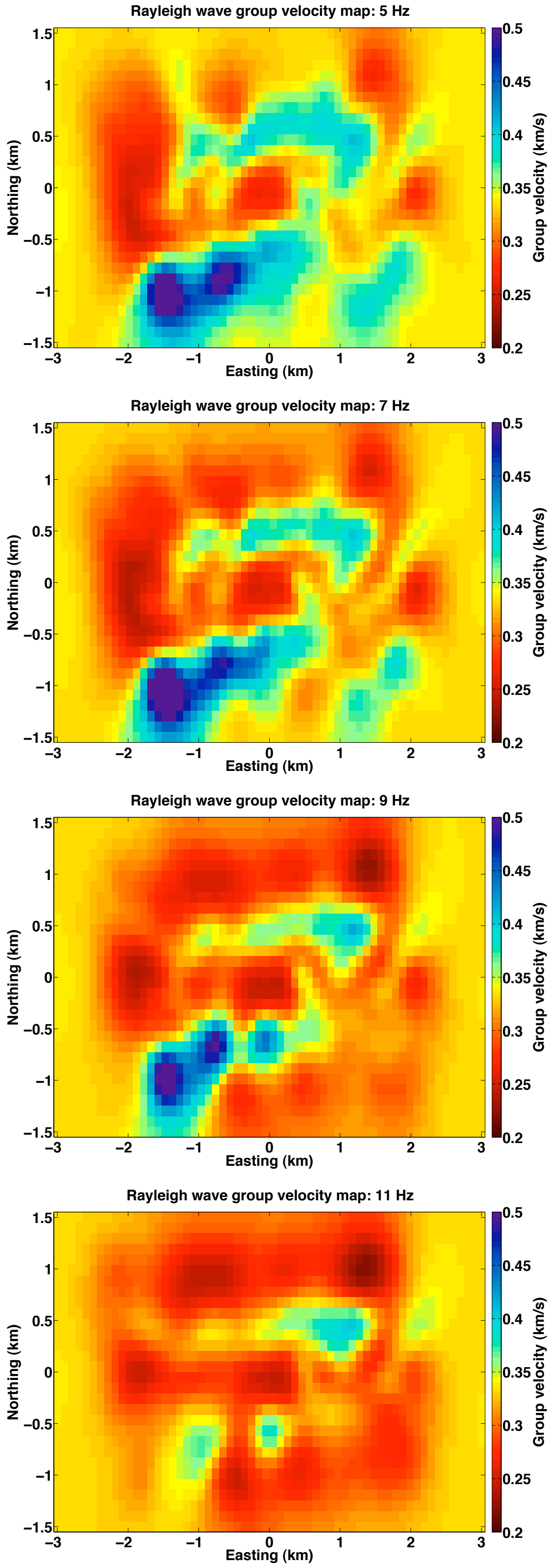

Figure 3: Group velocity maps for frequencies of 5 Hz (top), 7 Hz (upper middle), 9 Hz (lower middle), and 11 Hz (bottom).

For the tomography, we use the PRONTO code described by Aldridge and Oldenburg (1993). The algorithm is based on a finite-difference solution of the Eikonal equation and solves the inverse problem using a weighted-damped least-squares scheme. Originally designed for crosswell tomography, the 2D code is easily adapted to build surface wave group velocity maps. In fact, PRONTO has previously been used for Rayleigh wave group velocity tomography by Abbott et al. (2006) and Masterlark et al. (2010). The model of the Coronation Field employed by PRONTO consists of 60 x 30 cells in the east-west and north-south directions. Each cell is a square with sides 0.1 km in length.

RESULTS

In Figure 3, we plot several of the group velocity maps for the Coronation Field. On average, the tomography lowered the root-mean-squared error $\sim$ 15% relative to the initial laterally homogeneous model. The group velocities at lower frequencies are generally higher than at higher frequencies, as they should be for an increasing velocity trend with depth. Drainage patterns and elevation in the area of the Coronation Field are known to trend in the NE-SW direction (A. Calvert; personal communication 2009). The group velocity maps contain structures north of the receiver line that roughly trend in a ENE-WSW direction. The highest group velocities exist in the SW sector of the Coronation Field; however, resolution analysis presented in Figure 4 indicates that those velocities are poorly resolved. The most reliable structures are those close to the receiver line. The high velocity structure roughly 0.5 km north of the receiver line contrasts strongly with the lower group velocities nearby. Such a strong contrast in the near-surface should give rise to scattered surface waves, which have been observed in the field data during interactive data analysis on a workstation.

As pointed out, the resolution of the group velocity tomography for the subset of sources and receivers analyzed here is best in the vicinity of the receiver line. This can be seen in Figure 4, which shows the ray density for each cell and the result of a checkerboard test, respectively. The concentration of rays near the receiver line is clearly evident in the ray density map. Resolution can be further assessed with a synthetic checkboard test using 600 m x 600 m checkers. The checkers oscillate between high and low group velocity values of 350 m/s and 300 m/s. The righthand panel of Figure 4 shows that the region in which the checkers are reconstructed does not include the area with the highest group velocities in Figure 3.

DISCUSSION

The output of group velocity tomography is local group velocity as a function of the lateral coordinates and frequency - $u(x,y,f)$. The final step in 3D imaging of surface waves consists of inverting the local dispersion curves at each (x,y)-point for a local depth model of shear wave velocity. Masterlark et al. (2010) have recently applied this procedure for Rayleigh

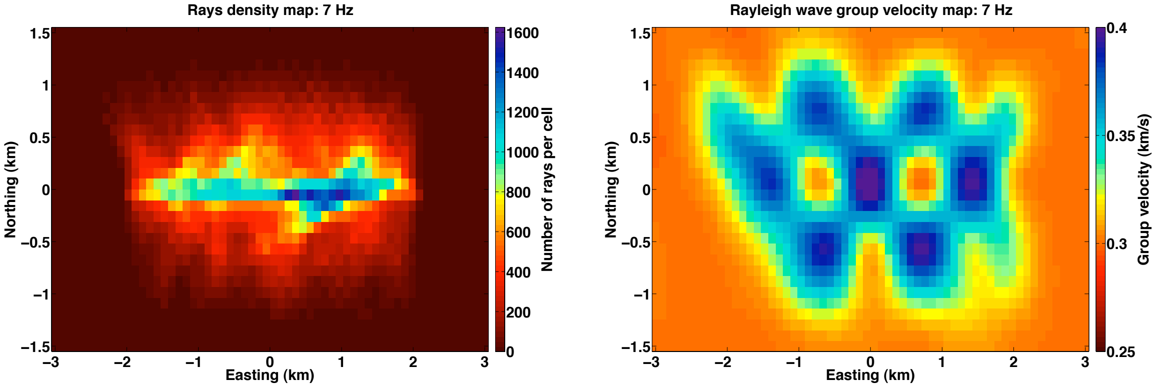

Figure 4: (left) The ray density for the group velocity tomography at 7 Hz. (right) A checkerboard resolution test involving 600 m x 600 m checkers.

wave data at Okmok Volcano and were able to image a shallow magma chamber centered at a depth of 4 km. We plan to similarly invert the collection of group velocity maps at Coronation Field for a 3D shear wave velocity model and compare the 3D model to shear wave statics obtained independently at the Coronation Field.

Other promising directions include the inversion of the first higher mode and HV ratio. The first higher mode can be observed on raw field records from the Coronation Field and offers the chance of resolving structure deeper than 100 m. The group velocity tomography approach demonstrated above can similarly be applied to the higher mode. Furthermore, HV ratio inversion is possible given the 3C data at the Coronation Field. HV ratio inversion would produce an image on a vertical plane defined by the receiver line. The HV ratio is theoretically a pure site effect and has no sensitivity to structure located laterally away from the receiver. On the other hand, it is not path-averaged like group velocity and therefore does not need to be untangled by applying tomography. As a result, the image produced by HV ratio would have smaller spatial extent but be of higher resolution.

CONCLUSION

We have successfully applied Rayleigh wave group velocity tomography to land data from the Coronation Field and imaged significant near-surface heterogeneity. The ability to estimate a shallow shear velocity model using surface waves offers a way to independently assess conventional shear wave statics. The smooth velocity models obtained from tomography can be used as initial models for more advanced surface wave analysis methods based on the full waveform. In this light, the techniques described in this abstract are a first step toward a more complete understanding of surface wave propagation and near surface structure at the Coronation Field.

ACKNOWLEDGMENTS

We thank ION Geophysical, in particular Alex Calvert, for providing the Coronation data set for this study.

EDITED REFERENCES

Note: This reference list is a copy-edited version of the reference list submitted by the author. Reference lists for the 2010 SEG Technical Program Expanded Abstracts have been copy edited so that references provided with the online metadata for each paper will achieve a high degree of linking to cited sources that appear on the Web.

REFERENCES

Abbott, R. E., L. C. Bartel, B. P. Engler, and S. Pullammanappallil, 2006, Surface-wave and refraction tomography at the FACT Site, Sandia National Laboratories, Albuquerque, New Mexico: Technical Report SAND20065098, Sandia National Laboratories.

Aldridge, D. F., and D. W. Oldenburg, 1993, Two-dimensional tomographic inversion with finite-difference traveltimes: Journal of Seismic Exploration, **2**, 257–274.

Bussat, S., and S. Kugler, 2009, Recording noise - estimating shear-wave velocities: Feasibility of offshore ambient noise surface-wave tomography (answt) on a reservoir scale: 79th Annual International Meeting, SEG, Expanded Abstracts, 1627–1631.

Masterlark, T., M. Haney, H. Dickinson, T. Fournier, and C. Searcy, 2010, Rheologic and structural controls on the deformation of Okmok volcano, Alaska: FEMs, InSAR, and ambient noise tomography: Journal of Geophysical Research, 115, B02409, doi:10.1029/2009JB006324.

Muyzert, E., 2007, Seabed property estimation from ambient noise recordings: Part 2 – Scholte-wave spectral-ratio inversion: Geophysics, **72**, no. 4, U47–U53, doi:10.1190/1.2719062.

Ritzwoller, M. H., and A. L. Levshin, 2002, Estimating shallow shear velocities with marine multicomponent seismic data: Geophysics, **67**, 1991–2004, doi:10.1190/1.1527099.

Ross, W. S., S. Lee, M. Diallo, M. L. Johnson, A. P. Shatilo, J. E. Anderson, and A. Martinez, 2008, Characterization of spatially varying surface waves in a land seismic survey: 78th Annual International Meeting, SEG, Expanded Abstracts, 2556–2560.

Xia, J., R. D. Miller, and C. B. Park, 1999, Estimation of near-surface shear-wave velocity by inversion of Rayleigh waves: Geophysics, **64**, 691–700, doi:10.1190/1.1444578.